Functional & Integrative Genomics (2026) 26:156
https://doi.org/10.1007/s10142-026-01942-9

RESEARCH

RHEBL1 expression is activated by the Oct4-Sox2 complex in oral squamous cell carcinoma

Feng Qiu[1,2] · Yaqiu Chen[2] · Peibo Li[1] · Zhuo Chen[3] · Alfred King-yin Lam[3,4] · Yuwei Liang[2] · Xiaojing Sun[5] · Qian Jiang[2] · Bin Qiao[3,6]

Received: 28 August 2025 / Revised: 10 June 2026 / Accepted: 11 June 2026

Abstract

RHEBL1 (RHEB2), a member of the Ras superfamily, has established roles in tumor-promoting signaling pathways including mTOR activation and NF-κB transcription; however, its specific role in oral squamous cell carcinoma (OSCC) and its regulation by the stem cell transcription factors Oct4 and Sox2 have not been previously characterized. This study aimed to elucidate the function and mechanism of RHEBL1 in OSCC development and analyze the regulatory influence of Oct4 and Sox2 on *RHEBL1* expression. Immunohistochemistry and immunofluorescence assessed RHEBL1, Oct4, and Sox2 expression in normal and precancerous tissues. *RHEBL1*-overexpressing and knockout cell lines were created for in vitro assessment of proliferation and self-renewal; mice models were used to evaluate tumor formation in vivo. Bioinformatics analyses predicted Oct4 and Sox2 binding sites within the *RHEBL1* promoter, validated by dual-luciferase reporter assays and ChIP-PCR. RHEBL1 showed high expression in OSCC and adjacent tissues, with linear arrangement of positive cells in the basal layer. High levels of RHEBL1, Oct4, and Sox2 were observed at the tumor invasion front and the basal layer of adjacent oral epithelia. RHEBL1 overexpression enhanced sphere formation and induced subcutaneous tumor-like lesions in immunodeficient mice, characterized histologically by invasive growth patterns and vascular structures, whereas control cells showed no such phenomenon. Furthermore, *RHEBL1* knockout significantly reduced in vitro sphere formation and in vivo tumorigenicity. Oct4-Sox2 complexes bound two sites in the *RHEBL1* promoter; mutations in these sites reduced transcriptional activation. Thus, this study demonstrated that Oct4 and Sox2 promote OSCC initiation and proliferation by regulating RHEBL1 expression. Clinical trial number**:** not applicable.

Keywords Oral squamous cell carcinoma · *RHEBL1* · *Oct4* · *Sox2* · Cancer stem cells

Feng Qiu and Yaqiu Chen contributed equally.

✉ Qian Jiang
200047@glmc.edu.cn

✉ Bin Qiao
qiaobin@zzu.edu.cn

[1] The Department of Stomatology, The First Affiliated Hospital of Zhengzhou University, No. 1 Jianshe East Road, Erqi District, Zhengzhou City, China

[2] The Department of Orthodontics, Affiliated Stomatology Hospital of Guilin Medical University, 109 Huancheng North 2nd Road, Qixing District, Guilin City, China

[3] Cancer Molecular Pathology of School of Medicine and Dentistry, Griffith University, Gold Coast, QLD 4222, Australia

[4] Faculty of Medicine, The University of Queensland, Herston, QLD 4006, Australia

[5] The Department of Orthodontics, Stomatology Hospital of Guilin, No. 5 Sanduo Road, Xiufeng District, Guilin, China

[6] Department of Oral and Maxillofacial Surgery, Dongguan Children's Hospital Affiliated to Guangdong Medica University/Dongguan Eighth Peoples Hospital, No. 68 South Xihu 3rd Road, Shilong Town, Dongguan, China

Published online: 23 June 2026

Introduction

Oral squamous cell carcinoma (OSCC) is one of the most devastating malignancies worldwide, with a 5-year survival rate of only 64.4% despite advances in treatment strategies (Zanoni et al. 2019; Al 2023). Although multiple risk factors have been identified, including genetic susceptibility, environmental factors, and viral infections (Chen et al. 2022; Gilligan et al. 2024), the molecular mechanisms underlying OSCC initiation and progression remain incompletely understood.

Recent studies have highlighted the critical role of the *Ras* superfamily in OSCC pathogenesis (Wang et al. 2012). Among them, RHEBL1 (also known as RHEB2), a member of the highly conserved *RHEB* family (Aspuria and Tamanoi 2004), has emerged as a potential key regulator in cancer development. RHEBL1 functions as a molecular switch in several crucial pathways: it activates mTOR signaling to promote cell growth (Tian et al. 2020; Sato et al. 2021; Xiao et al. 2020), stimulates c-Myc-mediated cell proliferation (Alevizopoulos et al. 1997), and enhances NF-κB transcriptional activity (Yuan et al. 2005). These functions contribute to tumor progression in various cancers, including renal clear cell carcinoma and leukemia (Bailey et al. 2014; Temraz et al. 2015). Additionally, RHEBL1 modulates cell survival through regulation of interferon regulatory factor 3, suggesting a role in tumor immune responses (Yu et al. 2023).

The transcription factors Oct4 and Sox2 regulate tumor-initiating cell maintenance (Yang et al. 2017), and their critical role is evidenced by embryonic lethality in *Oct4* or *Sox2* knockout mice. Oct4 (POU5F1), a *POU* family transcription factor, regulates stem cell differentiation during embryogenesis. It functions with endogenous Sox2 to reprogram mouse neural stem cells into induced pluripotent stem cells (Tsai et al. 2010).

Oct4 expression has been identified in OSCC and oral precancerous lesions (Qiao et al. 2014). Through its *POU* family homology domain, Oct4 binds specific DNA sequences to activate downstream targets. Sox2, a B1 subgroup member of the *Sox* family, is essential for embryonic development (Gao et al. 2024). Oct4 and Sox2 form a POU/HMG domain cassette that regulates fibroblast growth factor 4 (FGF4) transcription. This Oct4-Sox2 complex also forms a ternary structure with non-coding DNA sequences 2 kb upstream of the *RAX* promoter to enhance transcription (Grimm et al. 2020).

Our previous research established multiple cellular models, including *hTERT*$^+$-oral mucosal epithelial cell line (*hTERT*$^+$-OME), *hTERT*$^+$-*Oct4*$^+$-OME, *hTERT*$^+$-*Sox2*$^+$-OME, and *hTERT*$^+$-*Oct4*$^+$*Sox2*$^+$-OME, using gene transduction in oral cancer Cal27 cell lines (Qiao et al. 2012). With these genetically modified cells, this study aimed to investigate the mechanism of *RHEBL1* in OSCC development and the precise regulatory patterns of Oct4 and Sox2 on RHEBL1 expression, thereby providing new theoretical foundations for molecular diagnosis and targeted therapy.

Methods

Ethics statements

This study was approved by the Ethics Committee of Guilin Medical University (No: GLMC20240305) and conducted in accordance with the Declaration of Helsinki. All patients provided written informed consent for the collection and storage of their tissues for research purposes. In this study, the experimental animals were purchased from Beijing Weitong Lihua Experimental Animal Technology Co., Ltd., with the license number SCXK (Jing) 2016-0006. The mice used in the study were NOD-SCID mice and were housed in the specific pathogen free animal laboratory of the Basic Medical College of Zhengzhou University, at a temperature of 24 °C, relative humidity of 60%, and a 12 h/12 h light/dark cycle. All breeding and experimental procedures strictly followed the guidelines set by the Zhengzhou University Experimental Animal Ethics Committee.

Specimen collection

Clinical specimens included 40 non-neoplastic histological normal oral mucosa (NOM), 31 oral lichen planus (OLP), and 46 oral leukoplakia (OLK) cases from the Affiliated Stomatology Hospital of Guilin Medical University (ethical approval: GLMC20240305). Both OLP and OLK are classified as oral potentially malignant disorders (OPMDs) by the World Health Organization, associated with an elevated risk of malignant transformation compared with normal oral mucosa (WHO 2017). Although the transformation rate of OLP is lower than that of OLK, its inclusion in this study was intended to capture the full spectrum of potentially malignant changes oral changes and to examine early alterations in RHEBL1 expression across different stages of potential malignant progression. A commercial microarray (HOraC080PG01) containing 60 OSCC and precancerous mucosae samples was obtained from Shanghai Xinchao Biological Technology.

Cell culture and transfection

The *hTERT*$^+$-OME cell line was originally established and characterized by our group via retroviral transduction of primary human oral epithelial cells with the pLXSN-*hTERT*

vector (Qiao et al. 2012). Cal27 and HN4 cell lines were obtained from Shanghai Jiao Tong University (Shanghai, China), SCC15 and SCC25 from Sun Yat-sen University, and 293 T cells from Shanghai Jikai Gene Chemical Technology (Shanghai, China). Cal27 was selected as the primary OSCC model based on its well-characterized genetic background, robust growth properties, and its established utility in prior studies on oral carcinogenesis, including our previous work (Qiao et al. 2012). HN4, SCC15, and SCC25 cell lines were additionally employed to validate RHEBL1 expression patterns and ChIP-PCR binding results, ensuring cross-validation of key findings across multiple OSCC cell backgrounds.Cells were cultured in DMEM/F12 (Biological Industries, Beit-Haemek, Israel) or high-glucose DMEM (Biological Industries) supplemented with 10% fetal bovine serum and antibiotics at 37 °C with 5% CO_2.

Bioinformatic analysis

Transcriptomic analyses were based on RNA sequencing data generated in our previous work (Gilligan et al. 2024), performed on two complementary cell model pairs: hTERT$^+$-OME versus hTERT$^+$-O$^+$S$^+$-OME (Oct4/Sox2 overexpression model), and Cal27 versus Cal27-O^{low}S^{low} (Oct4/Sox2 knockdown model). In the current study, these datasets were re-analyzed to identify downstream targets of Oct4/Sox2. Hierarchical clustering analysis was performed using FPKM values normalized by $\log_{10}(\text{FPKM}+1)$ to visualize differential mRNA expression patterns across cell groups, with bioinformatics assistance provided by Novogene Co., Ltd. (Beijing, China). Differentially expressed genes (DEGs) were identified using volcano plots of $\log_2(\text{RPKM}+1)$ values against $-\log_{10}(P\text{-value})$, with a significance threshold of $P<0.05$ and fold change ≥ 2. Genes showing consistent and directionally opposite regulation across both the overexpression and knockdown models were selected as candidate Oct4/Sox2 downstream targets.

Gene and protein expression analysis

RHEBL1 promoter sequences were analyzed using NCBI, UCSC, and JASPAR databases. RT-qPCR was performed using standard protocols, with *GAPDH* as an internal control. For western blotting, proteins were extracted from OSCC cells and tumors using RIPA buffer with protease inhibitors and quantified by the bicinchoninic acid method. Samples (50 µg) were separated using 10% sodium dodecyl sulfate–polyacrylamide gel electrophoresis and transferred to polyvinylidene difluoride membranes. After blocking with 5% skim milk, membranes were incubated with primary antibodies (anti-RHEBL1, anti-Oct4, and anti-Sox2 at 1:1000; anti-GAPDH at 1:5000) overnight at 4 °C, followed by secondary antibody incubation for 1 h. Visualization was performed using an enhanced chemiluminscence kit.

Regarding ChIP-PCR analysis, formaldehyde-crosslinked cells were lysed, sonicated, and centrifuged. Supernatants were incubated with Oct4 or Sox2 antibodies and magnetic beads overnight. After washing, chromatin complexes were de-crosslinked (62 °C, 2 h), purified, and analyzed using qPCR.

RIPA lysis buffer (Solarbio, Beijing, China); protease inhibitor cocktail (Sigma/Merck, Darmstadt, Germany); anti-RHEBL1 antibody (Santa Cruz Biotechnology, Dallas, TX, USA); anti-Oct4 and anti-Sox2 antibodies (R&D Systems, Minneapolis, MN, USA); anti-GAPDH antibody (Proteintech, Rosemont, IL, USA); HRP-conjugated secondary antibodies (ZSGB-BIO, Beijing, China); ECL kit (Solarbio, Beijing, China); imaging performed on an iBright Imaging System (Thermo Fisher Scientific, Waltham, MA, USA); RT-qPCR performed on an ABI 7500 Fast Real-Time PCR System (ABI/Thermo Fisher Scientific) with Real Time PCR Mixture (Cofitt, China).

Gene regulation and functional validation assaysCRISPR-dCas9 system

For RHEBL1 overexpression, a CRISPRa-based SAM (synergistic activation mediator) dual-vector system was employed: three sgRNAs targeting the RHEBL1 promoter region were cloned into lentiviral vector GV468 (U6-sgRNA-SV40-MS2-P65-HSF1-CMV-EGFP) and co-delivered with a pre-validated dCas9-VP64 lentiviral vector (Lenti-dCAS9-VP64-Puro; Shanghai Jikai Gene Chemical Technology, Shanghai, China) to transcriptionally activate endogenous RHEBL1 without altering the genomic sequence. For RHEBL1 knockout in Cal27 cells, a standard CRISPR-Cas9 system was used with three independent sgRNAs cloned into lentiviral vector GV392 (U6-sgRNA-EF1a-Cas9-FLAG-P2A-puro; Shanghai Jikai Gene Chemical Technology), delivered at a multiplicity of infection of 10. Oct4 and Sox2 knockdown in Cal27 cells was achieved using lentiviral shRNA constructs targeting POU5F1 and SOX2; overexpression in hTERT$^+$-OME cells used lentiviral vectors carrying full-length POU5F1 and SOX2 coding sequences under a CMV promoter, as described previously (Qiao et al. 2012). Stable cell lines were selected using puromycin (10 µg/mL for 7 days, reduced to 2.5 µg/mL for maintenance); the SAM overexpression system was additionally verified by FACS sorting of EGFP-positive cells. All stable lines were confirmed by Western blot. sgRNA sequences are provided in Supplementary Table 6. The fidelity of all promoter mutation constructs (promoter-MUT1 and promoter-MUT2) was confirmed by Sanger sequencing prior to transfection and functional assays.

Lentiviral constructs used the GV712 vector (Genechem, Shanghai, China); luciferase reporter assays used the Dual-Luciferase® Reporter Assay System (Promega, Madison, WI, USA); transfection performed with X-tremeGENE HP DNA Transfection Reagent (Roche); luciferase activity measured on a GloMax luminometer (Promega).

3D sphere formation assay

Cells (5000/mL) were cultured in DMEM/F12 supplemented with bFGF (20 ng/mL), EGF (20 ng/mL), B27 (1:50), and heparin (4 g/mL) in low-adhesion plates. Sphere formation was evaluated after 5–7 d. bFGF (PeproTech/Thermo Fisher Scientific); EGF (PeproTech); B27 supplement (Thermo Fisher Scientific); heparin sodium (Sigma-Aldrich/Merck, Darmstadt, Germany); ultra-low attachment plates (Corning, Corning, NY, USA). Spheres with diameter > 100 μm were counted using an inverted microscope, and sphere formation efficiency was calculated as the percentage of seeded cells forming spheres.

In vivo tumor formation

Female NOD-SCID mice (Beijing Weitong Lihua Laboratory Animal Technology, Beijing, China) were maintained under standard conditions (24 °C, 60% humidity, 12-h light–dark cycle) following institutional ethical guidelines.

The mice (4 weeks, $n = 20$) were divided into four groups. Stably transfected cells were cultured in sphere-forming medium for 3 d then adjusted to 5×10^7 cells/mL and mixed 1:1 with Matrigel. Each mouse received 200 μL (5×10^6 cells) subcutaneously. Tumor measurements were taken every 3 d for 31 d before harvest and fixation.

Matrigel was purchased from BD Biosciences (Franklin Lakes, NJ, USA). Tumor volume was calculated using the formula $V = (\text{length} \times \text{width}^2)/2$.

Immunohistochemistry and multi-label immunofluorescence

Standard immunohistochemistry was performed as follows: 5-μm paraffin sections were processed using universal kits (ZSGB-BIO, Beijing, China). After antigen retrieval and blocking, sections were incubated with primary antibodies (4 °C, overnight) and secondary antibodies (room temperature, 30 min), followed by DAB and hematoxylin staining. Multi-label immunofluorescence followed similar preparation steps with additional counterstaining to enable simultaneous detection of multiple targets. Immunofluorescence was performed using Alexa Fluor-conjugated secondary antibodies (Thermo Fisher Scientific). All clinical specimens were histologically reviewed and categorized by a certified pathologist according to WHO criteria. Precancerous lesions (OLP and OLK) were diagnosed based on established clinical and histological features. Epithelial dysplasia was noted where present but was not further graded in the current analysis, which represents a limitation that should be addressed in future studies with larger, dysplasia-graded cohorts.

Statistical analysis

Sample sizes were determined using a power analysis ($\alpha = 0.05$, power = 80%) based on preliminary data. Animal studies include 5 animals per group; cell culture experiments used 3–6 replicates based on observed variance. Mice were randomly assigned to the groups using computer-generated sequences. Investigators were blinded to group assignments during data collection and analysis. Clinical specimens were coded and scored by a blinded pathologist. Cell culture experiments used random allocation to treatment conditions. The inclusion criteria were: histologically confirmed samples, adequate tissue quality, and cell viability > 95%. The exclusion criteria were: previous therapy (clinical samples), contamination (cell cultures), illness (animals). Statistical analysis was performed using GraphPad Prism 8 (GraphPad Software, San Diego, CA, USA), with $P < 0.05$ considered statistically significant. For comparisons between two groups, Student's unpaired t-test was used. For comparisons among three or more groups, one-way analysis of variance (ANOVA) followed by Tukey's post hoc test was applied. The Kruskal-Wallis test was used for non-normally distributed data. Chi-squared test was used for categorical data comparisons (e.g., immunohistochemistry scores between tissue groups). All cell culture experiments were performed in triplicate unless otherwise stated, and results are presented as mean ± standard deviation (SD).

Results

Transcriptome analysis identifying RHEBL1 as a potential downstream target of Oct4/Sox2

Based on previous findings, this study aimed to identify the downstream targets of Oct4/Sox2 using transcriptome analysis. Two complementary cell models were established: Cal27 cells with *Oct4/Sox2* knockdown (Cal27-OS^{low}) and immortalized oral epithelial cells with Oct4/Sox2 overexpression ($hTERT^{+}$-OS^{+}). This dual-model strategy was designed to minimize cell-line-specific confounding: genes showing consistent regulation in opposite directions across both the overexpression and knockdown systems are more likely to represent genuine Oct4/Sox2 downstream targets rather than artifacts of a single cellular background.

Hierarchical clustering analysis (fold change ≥ 2, $P < 0.05$) revealed distinct gene expression profiles in both models (Fig. 1A). In *hTERT*$^{+}$-OME cells, Oct4/Sox2 overexpression led to differential expression of 101 transcripts (54 upregulated, 47 downregulated; Fig. 1B). A more pronounced effect was observed in the knockdown cells, with 1,422 altered transcripts (207 upregulated, 1,215 downregulated; Fig. 1B).

Genes showing consistent regulation patterns across both models were selected to identify the most reliable Oct4/Sox2 targets. This comparative analysis identified 19 transcripts (Fig. 1C, Supplementary Table 1). Among these, RHEBL1 showed the most significant changes and opposite regulation patterns: upregulated by Oct4/Sox2 overexpression but downregulated by *Oct4/Sox2* knockdown, suggesting that it is a key downstream target of Oct4/Sox2 signaling.

RHEBL1 expression in cell groups, normal oral mucosa, and precancerous lesions

To validate the transcriptome findings, RHEBL1 expression was first examined in vitro and in clinical samples. In cell models, RT-qPCR analysis confirmed that RHEBL1 mRNA levels were positively regulated by Oct4/Sox2: overexpression of Oct4 and/or Sox2 increased RHEBL1 expression in oral epithelial cells, whereas their silencing in Cal27 cells showed the opposite effect (Fig. 2A, B).

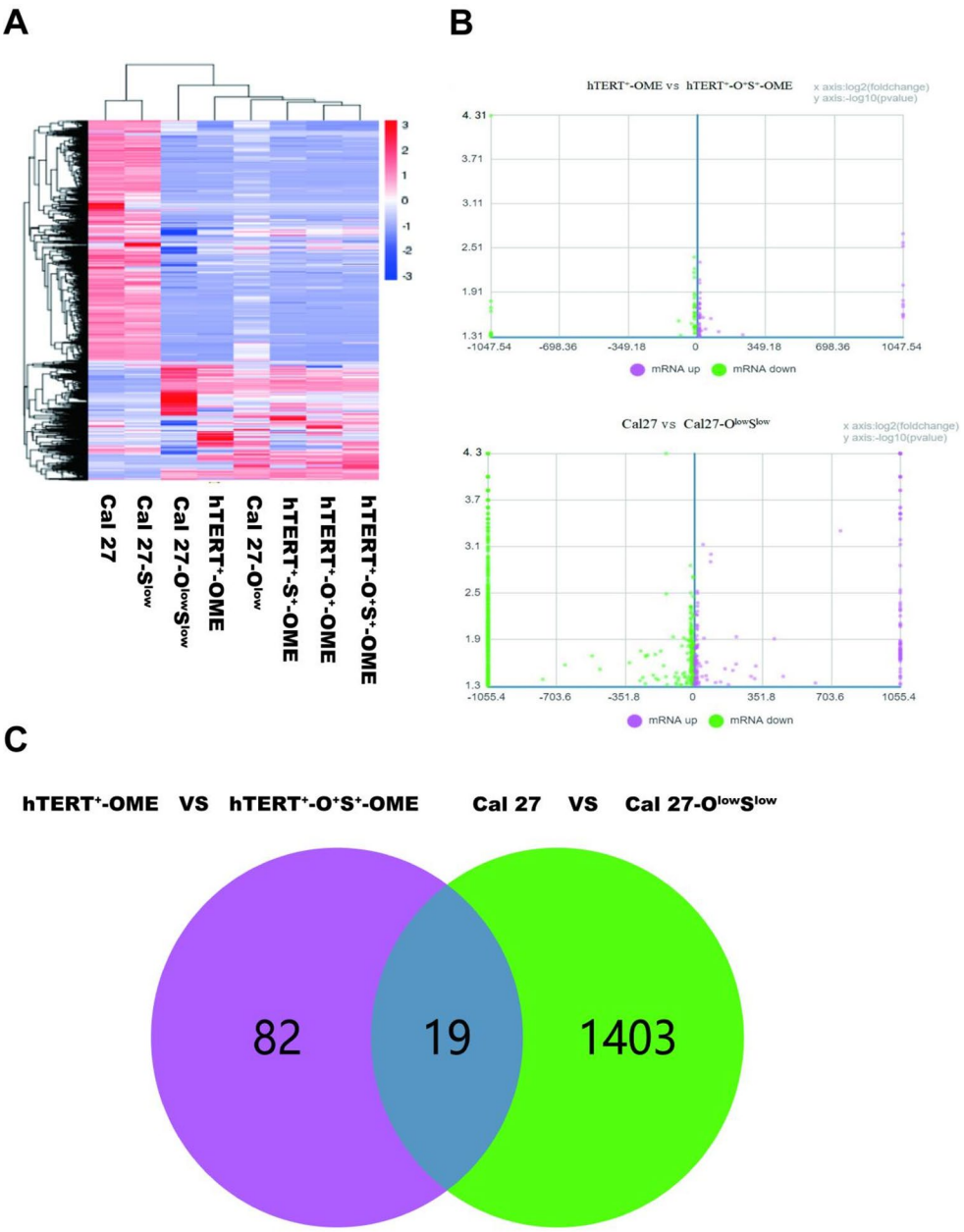

Fig. 1 Transcriptome analysis identifying RHEBL1 as a top candidate downstream target of Oct4/Sox2. (**A**) The overall FPKM hierarchical clustering map, clustered by $\log_{10}(\text{FPKM}+1)$ value; red indicates highly expressed genes, and blue indicates minimally expressed genes. (**B**) Volcano diagram of differential transcripts: mRNA up (upregulated transcripts) and mRNA down (downregulated transcripts). The x-axis is the difference in expression, and the y-axis is the p-value. (**C**) Shared transcripts in the differential transcripts between the *hTERT*$^{+}$-OME and *hTERT*$^{+}$-$O^{+}S^{+}$-OME groups and between the Cal27 and Cal27-$O^{low}S^{low}$ groups

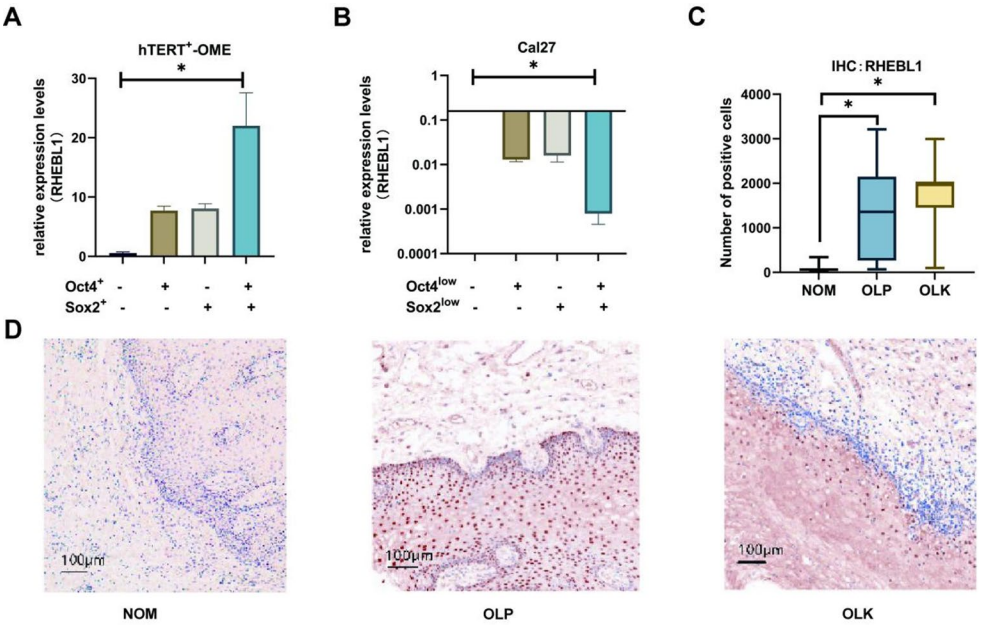

Fig. 2 Expression of RHEBL1 in each group of cells, from normal and precancerous oral mucosa tissues. (**A**) *RHEBL1* mRNA expression in *hTERT*$^{+}$-OME cells. (**B**) *RHEBL1* mRNA expression in Cal27 cells. (**C**) Analysis of immunohistochemical staining for RHEBL1. (**D**) Representative images of immunohistochemical staining for RHEBL1 in histological normal oral mucosa (NOM), oral leukoplakia (OLK), and oral lichen planus (OLP)

Table 1 RHEBL1 expression in clinical oral cancer samples

Group	Positive	Negative
NOM	0 (0)	40 (100)
OLP	14 (45.2)	17 (54.8)
OLK	28 (60.9)	18 (39.1)

Data are presented as number (%)

NOM histologically normal oral mucosa, *OLP* oral lichen planus, *OLK* oral leukoplakia

The subsequent immunohistochemistry analysis using clinical specimens included 40 NOM, 31 OLP, and 46 OLK samples. RHEBL1 staining was evaluated based on the Immunoreactive Score system, which combines staining intensity (0: negative; 1: weak; 2: moderate; 3: strong) and percentage of positive cells (0: none; 1: <10%; 2: 10–50%; 3: 51–80%; 4: >80%), resulting in a final score ranging from 0 to 12. NOM tissues showed minimal RHEBL1 expression, whereas positive staining was observed in OLP (45.2%) and OLK (60.9%) samples. Notably, RHEBL1-positive cells exhibited a distinctive linear arrangement in the basal layer of OPMD lesions, a pattern that warrants further investigation in relation to early oncogenic events (Table 1; Fig. 2D). Statistical analysis confirmed significantly higher RHEBL1 expression in OLP and OLK groups compared with NOM ($P<0.05$), although no significant difference was found between OLP and OLK groups (Fig. 2C).

RHEBL1, Oct4, and Sox2 expression in OSCC tissues

Once the correlation between RHEBL1 expression and precancerous progression was established, the spatial relationship between RHEBL1, Oct4, and Sox2 was subsequently investigated. Multi-label immunofluorescence was performed on 60 paired OSCC and peritumoral tissue samples, revealing distinct co-expression patterns of these three proteins.

In peritumoral epithelia, *RHEBL1*$^{+}$*/Oct4*$^{+}$*/Sox2*$^{+}$ cells (20% of total cells) predominantly exhibited a linear arrangement in the basal layer (Fig. 3A, B), consistent with the findings in precancerous lesions. In OSCC tissues, these triple-positive cells (25% of total cells) were concentrated within cancer nests adjacent to the stromal compartment (Fig. 3C, D), suggesting their potential involvement in tumor-stromal interactions. The distribution patterns between peritumoral and OSCC tissues were significantly different ($P<0.05$).

The specific localization of triple-positive cells in the basal layer of peritumoral tissue and the invasive front of OSCC suggests a potential role for the Oct4-Sox2-RHEBL1 axis in tumor initiation and progression.

RHEBL1 overexpression enhances hTERT^{+}-OME cell proliferation

To investigate the functional significance of RHEBL1 in oral epithelial cell oncogenic reprogramming and tumorigenic induction, RHEBL1-overexpressing cell models were established. Three different sgRNA vectors targeting *RHEBL1* were introduced into *hTERT*$^{+}$-OME cells, with *hTERT*$^{+}$-*RHEBL1*$^{+}$-OME-2 showing the highest RHEBL1 expression (Fig. 4B, C); this cell line was selected for subsequent experiments (designated as *hTERT*$^{+}$-*RHEBL1*$^{+}$-OME).

The impact of RHEBL1 overexpression on cellular phenotype was evaluated using sphere formation assays, a well-established method for assessing stem-like properties. Under serum-free, low-attachment conditions,

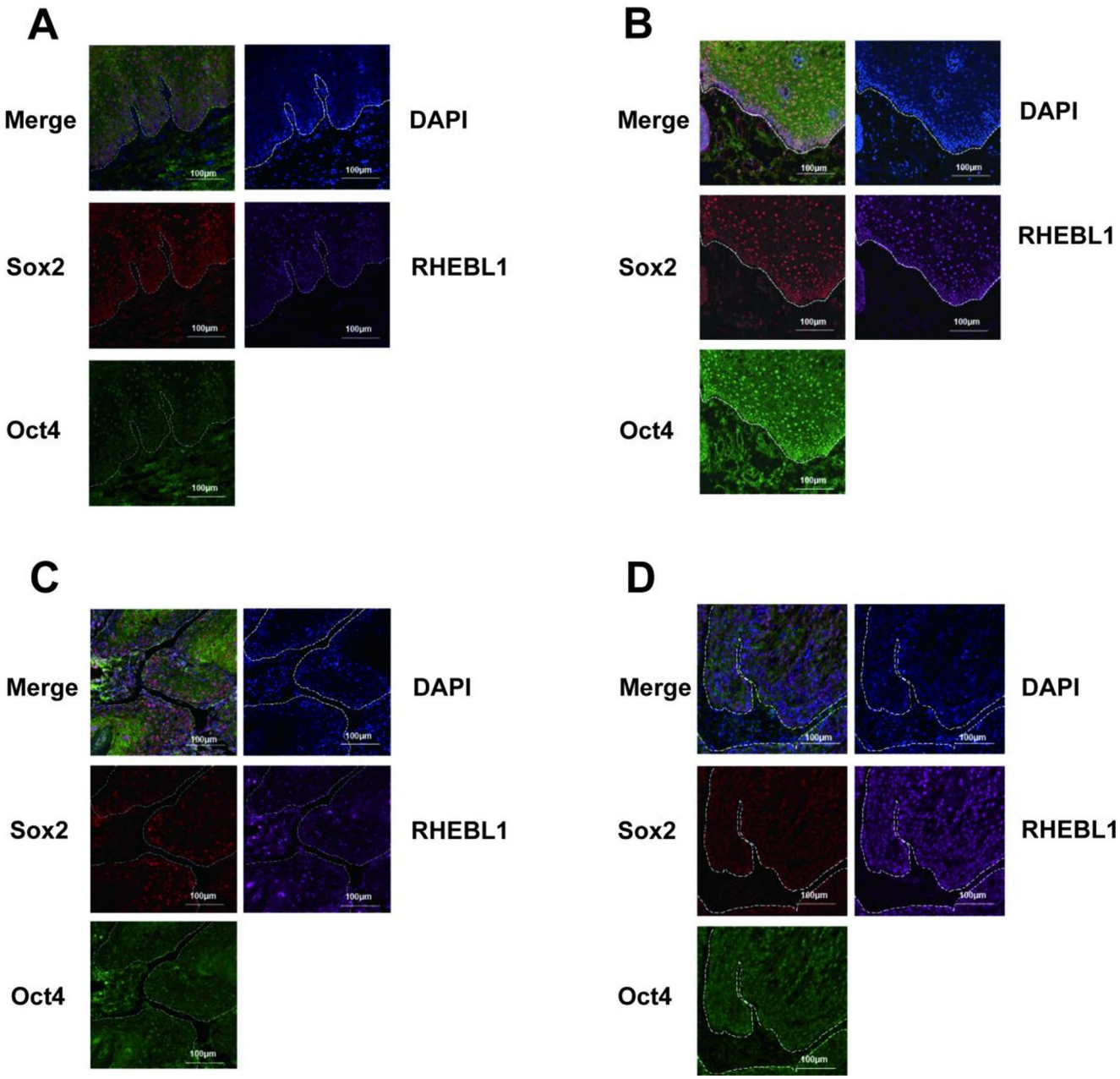

Fig. 3 Expression of RHEBL1, Oct4, and Sox2 in OSCC and paracancerous tissues. (**A**) Peritumoral tissue. (**B**) Peritumoral tissue. (**C**) OSCC tissue. (**D**) OSCC tissue

hTERT^{+}-*RHEBL1*$^{+}$-OME cells formed significantly more microspheres (>100 μm, average 12/well) than control cells after 7 days of culture ($P<0.05$, Fig. 4D, E).

Interestingly, RHEBL1 expression showed culture condition-dependent patterns. While consistently higher in *hTERT*$^{+}$-*RHEBL1*$^{+}$-OME cells under both 2D ($P<0.05$) and 3D ($P<0.01$) conditions, control cells exhibited spontaneous RHEBL1 upregulation specifically in 3D culture ($P<0.05$, Fig. 4F, G), suggesting a potential role for RHEBL1 in spheroid formation.

To assess tumorigenic potential, subcutaneous transplantation experiments were performed in immunodeficient mice ($n=5$ per group). All mice receiving *hTERT*$^{+}$-*RHEBL1*$^{+}$-OME cells developed tumors (three independent replicates: 0.085 g/72 mm^3, 0.041 g/47 mm^3, and 0.075 g/66 mm^3), whereas no tumors were observed in the control group (Fig. 4H, J, K). Histopathological examination revealed that these RHEBL1-induced tumors shared key features with *Oct4/Sox2*-induced tumors, including muscle invasion and morphologically apparent vascular structures within the lesions, as observed on H&E-stained sections (Fig. 4I). Formal quantification of neovascularization using endothelial markers such as CD31 was not performed in this study and

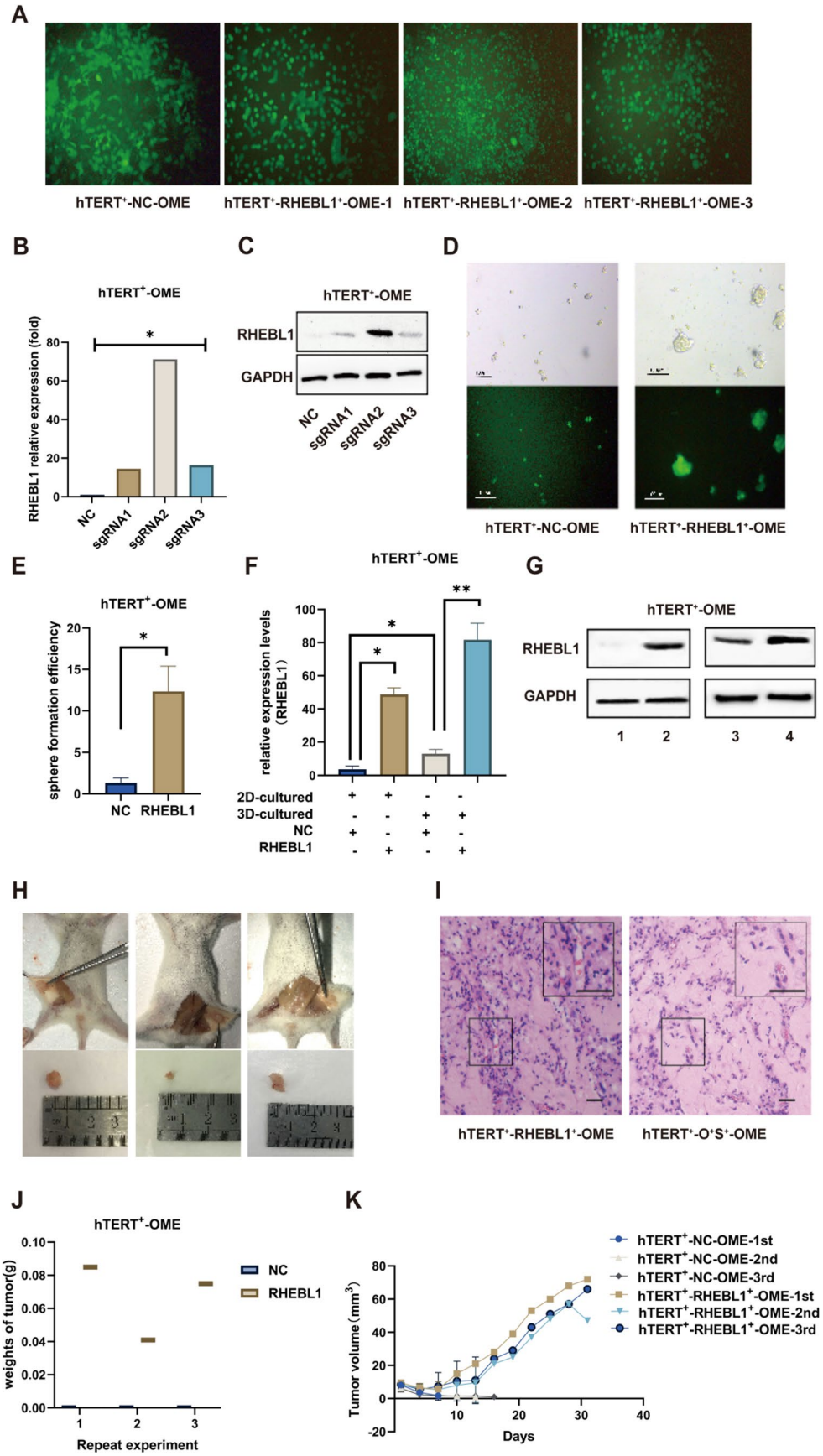

Fig. 4 Effect of RHEBL1 overexpression on immortalized oral epithelial *hTERT*$^{+}$-OME cells. (**A**) Cell lines purified by flow cell sorting technique. (**B**) Expression of RHEBL1 in purified cell lines using qPCR. (**C**) Expression of RHEBL1 in purified cell lines using western blot. (**D**) The *hTERT*$^{+}$-*RHEBL1*$^{+}$-OME cells formed microspheres greater than 100 μm. (**E**) The *hTERT*$^{+}$-*RHEBL1*$^{+}$-OME sphere formation efficiency was significantly higher than that in the control group. (**F**) qPCR verified the differential expression of RHEBL1 in *hTERT*+-*RHEBL1*$^{+}$-OME and *hTERT*$^{+}$-NC-OME cells under different culture conditions, **P*<0.05, ***P*<0.01. (**G**) Western blot verifying the differential expression of RHEBL expression in *hTERT*$^{+}$-*RHEBL1*$^{+}$-OME and *hTERT*$^{+}$-NC-OME cells under different culture conditions (1: 2D *hTERT*$^{+}$-NC-OME cells, 2: 2D *hTERT*$^{+}$-*RHEBL1*$^{+}$-OME cells, 3: 3D *hTERT*$^{+}$-NC-OME cells, and 4: 3D *hTERT*$^{+}$-*RHEBL1*$^{+}$-OME cells). (**H**) In vivo tumor formation of *hTERT*$^{+}$-*RHEBL1*$^{+}$-OME in combined immunodeficiency (NOD-SCID) mice in three independent replicate experiments. (**I**) The tumor-like lesions formed by *hTERT*$^{+}$-*RHEBL1*$^{+}$-OME and *hTERT*$^{+}$-*O*$^{+}$*S*$^{+}$-OME showed neovascularization. (**J**) Tumor weights from hTERT^{+}-RHEBL1^{+}-OME and hTERT^{+}-NC-OME cells in three independent replicate experiments ($n=5$ mice per group per replicate). Each point represents the mean tumor weight of one independent replicate. (**K**) Lesion volume formed by *hTERT*$^{+}$-*RHEBL1*$^{+}$-OME in mice in three independent replicates.Each point represents the mean tumor volume of one independent replicate; error bars represent SD across replicate means

should be addressed in future work. These findings nonetheless suggest that RHEBL1 may partly mediate the oncogenic effects of Oct4/Sox2.

RHEBL1 knockout reduces Cal27 cell tumorigenicity

Cal27-*RHEBL1*$^{K.O}$ cells were established using three independent sgRNAs targeting *RHEBL1*, with a scrambled sgRNA serving as control. Western blot analysis revealed that Cal27-*RHEBL1*−2 showed the most efficient *RHEBL1* knockout; this line was selected for subsequent experiments (Fig. 5A, B).

In vitro sphere formation assays demonstrated that Cal27-*RHEBL1*$^{K.O}$ cells formed significantly fewer and smaller spheres than controls (4.2 ± 0.8 vs. 12.5 ± 1.2 spheres/well, $P < 0.01$, Fig. 5C, D).

For in vivo tumorigenicity assessment, cells were subcutaneously injected into NOD-SCID mice ($n = 5$ per group). Although both groups developed tumors, Cal27-*RHEBL1*$^{K.O}$-derived tumors were significantly smaller in both weight (0.146 g vs. 0.300 g, 51.3% reduction) and volume (116.8 mm^3 vs. 390.1 mm^3, 70.1% reduction) compared with controls (Fig. 5E-G). Histological analysis

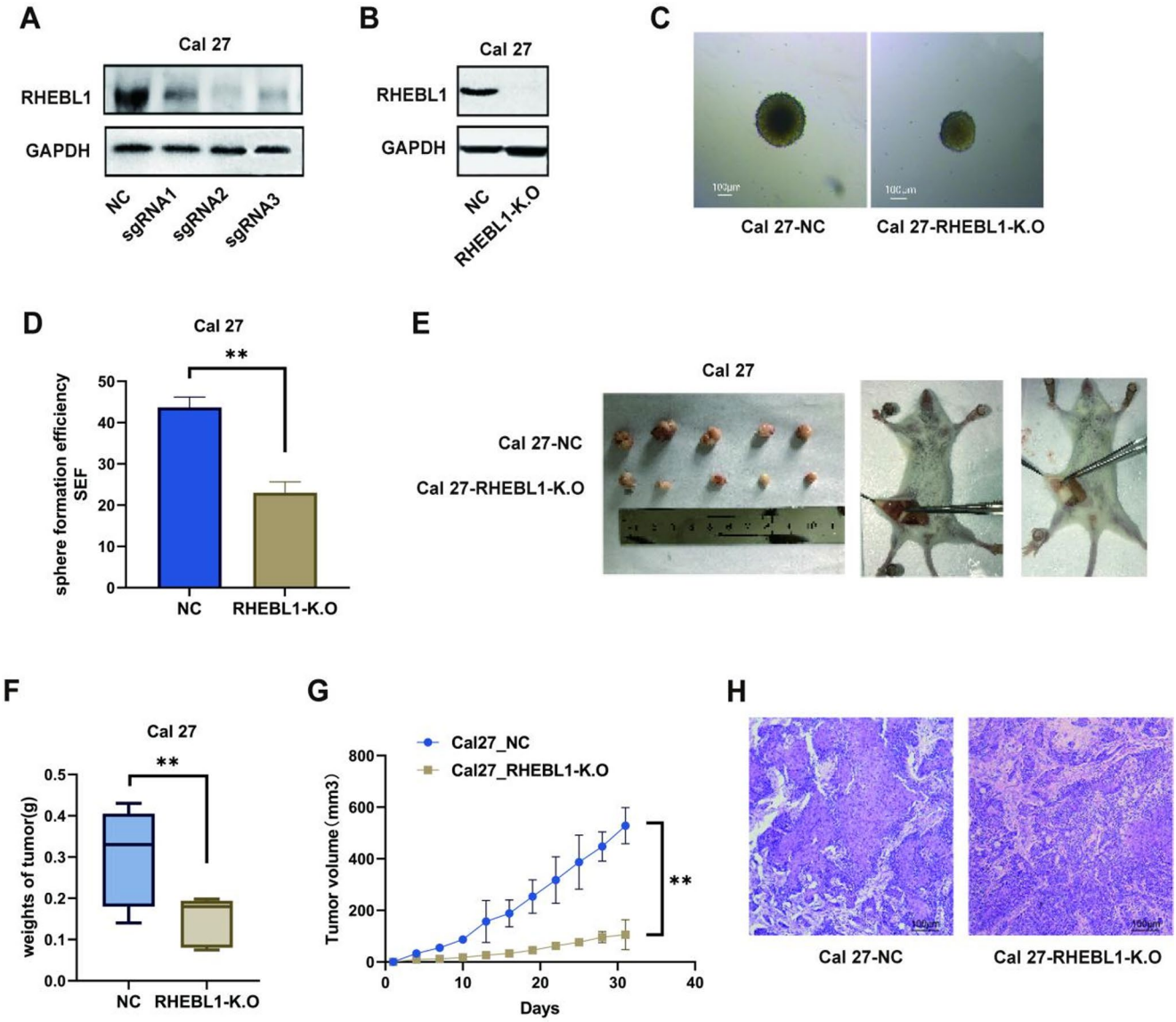

Fig. 5 Effect on OSCC Cal27 cells after knocking down *RHEBL1*. (**A**) Western blot was used to verify the *RHEBL1* knockdown efficiency of each group of cells. (**B**) Western blot verified that *RHEBL1* was completely knocked down in the monoclonal cell lines. (**C**) Differences in the in vitro spheroid volume between Cal27-*RHEBL1*$^{K.O}$ and Cal27-NC. (**D**) Differential in vitro sphere formation efficiency between Cal27-*RHEBL1*$^{K.O}$ and Cal27-NC, $^{**}P < 0.01$. (**E**) The tumorigenic ability of the Cal27-*RHEBL1*$^{K.O}$ group was significantly decreased. (**F**) Significant difference in tumor weight between Cal27-*RHEBL1*$^{K.O}$ and Cal27-NC cell groups, $^{**}P < 0.01$. (**G**) The difference in tumor volume between Cal27-*RHEBL1*$^{K.O}$ and Cal27-NC cells was statistically significant, $^{**}P < 0.01$. (**H**) Hematoxylin-eosin staining of tumor samples formed by Cal27-NC and Cal27-*RHEBL1*$^{K.O}$

confirmed that tumors from both groups maintained typical squamous cell carcinoma features, including keratinization and invasive growth patterns (Fig. 5H).

Oct4 and Sox2 cooperatively regulate RHEBL1 transcription

To investigate the molecular mechanisms of *RHEBL1* regulation by Oct4 and Sox2, its promoter region was analyzed. Using NCBI and UCSC databases, a 2,000-bp regulatory sequence was identified upstream of the *RHEBL1* coding region and contained multiple conserved transcription factor binding sites (Supplementary File 1). Bioinformatic analysis using JASPAR revealed two potential Oct4-Sox2 complex (MA0142.1) binding sites within this region (positions −1576/−1556 and −876/−856, Supplementary Table 2). To validate these sites, wild-type and mutant *RHEBL1* promoter constructs were generated by substituting key nucleotides within the predicted binding motifs (Fig. 6C, Supplementary File 2).

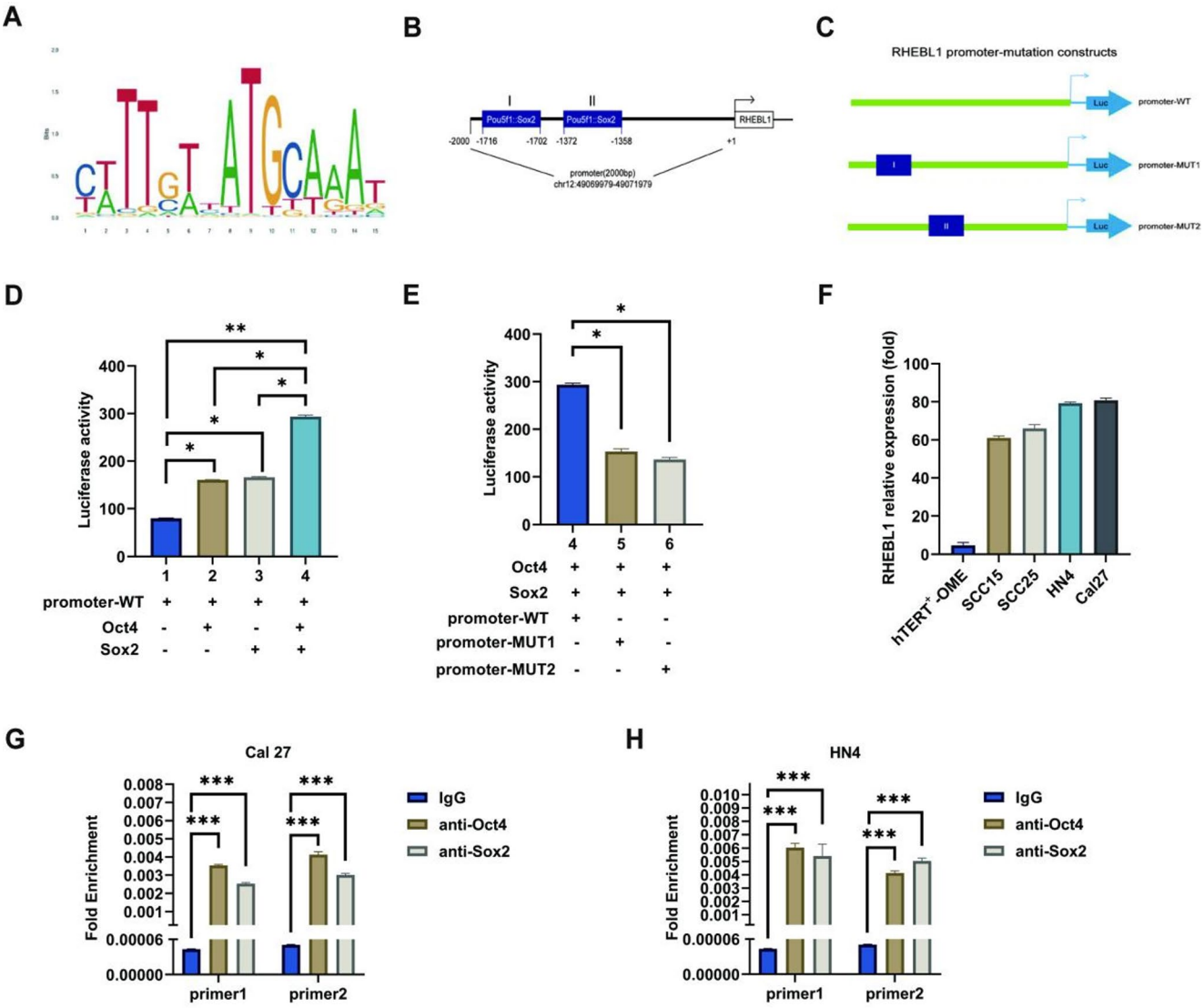

Fig. 6 Oct4 and Sox2 can cooperatively promote *RHEBL1* gene transcription. (**A**) Oct4-Sox2 complex (Pou5f1:Sox2, ID: MA0142.1). (**B**) The binding sites I and II of the Oct4-Sox2 complex in the promoter region of *RHEBL1*. (**C**) Schematic diagram of the *RHEBL1* promoter region: wild-type and mutant overexpression vector structures; I and II are the mutation positions of Oct4-Sox2 complex (Pou5f1::Sox2, ID: MA0142.1). (**D**) Both Oct4 and Sox2 can independently promote *RHEBL1* transcription, $*P<0.05$. Oct4 and Sox2 co-expression showed the strongest transcription facilitation of *RHEBL1*, $*P<0.01$. In panel D, lane 1 represents cells transfected with promoter-WT and empty expression vector (mock), serving as the baseline control. In panel E, luciferase activity of each mutant construct is normalized to the wild-type promoter with Oct4 + Sox2 co-transfection condition. (**E**) Mutant fluorescence expression was decreased compared with wild-type, $*P<0.05$. (**F**) Expression levels of RHEBL1 in each cell type. (**G**) Both the primer1 and primer2 primer fragments in Cal27 cells were amplified in the ChIP products of Oct4 and Sox2. (**H**) Both the primer1 and the primer2 primer fragments in HN4 cells were amplified in the ChIP products of Oct4 and Sox2

Promoter activity assays in 293 T cells demonstrated that Oct4 or Sox2 alone increased luciferase activity by 2.3-fold and 2.8-fold, respectively ($P<0.05$), whereas their co-expression led to a 4.7-fold increase ($P<0.01$; Fig. 6D), demonstrating cooperative transcriptional activation that exceeds the effect of either factor alone. Mutation of either binding site significantly reduced promoter activation by Oct4-Sox2 (decreased by 65% and 58%, $P<0.05$, Fig. 6E).

To confirm direct binding of Oct4 and Sox2 to the *RHEBL1* promoter in OSCC cells, ChIP-PCR was performed in HN4 and Cal27 cells, showing high endogenous RHEBL1 expression (Fig. 6F). Using site-specific primers (Supplementary Table 4), significant enrichment of both binding regions was detected in Oct4 and Sox2 immunoprecipitants (8.5-fold and 7.2-fold over IgG control, $P<0.005$, Fig. 6G, H).

Discussion

Using a systematic comparative transcriptome analysis, *RHEBL1* was identified as a critical downstream target of Oct4 and Sox2 signaling. This study demonstrated that Oct4 and Sox2 cooperatively activate RHEBL1 expression by binding to two specific sites in its promoter, thus establishing a direct regulatory relationship between stem cell transcription factors and a member of the *Ras* superfamily. This finding significantly expands our understanding of how these pluripotency factors promote OSCC development. Although previous studies have demonstrated the co-expression of Oct4 and Sox2 in OSCC and precancerous lesions (Qiao et al. 2014), this study established a clear mechanistic link between these stem cell transcription factors and RHEBL1. Furthermore, identifying RHEBL1 as a key mediator in the Oct4/Sox2 regulatory network is particularly significant given the established role of the *Ras* superfamily in OSCC pathogenesis (Wang et al. 2012).

To better understand the clinical relevance of this regulatory axis, a comprehensive analysis of RHEBL1 expression was conducted across the spectrum of oral carcinogenesis. When examining normal, precancerous, and malignant oral tissues, RHEBL1 expression was found to be higher in OPMD lesions (OLP and OLK) and OSCC than in normal oral mucosa, with the difference in positivity rate between OLK (60.9%) and OLP (45.2%) paralleling the recognized differences in malignant transformation potential between these two OPMD subtypes (Liu et al. 2025). Whether RHEBL1 upregulation is causally linked to dysplastic progression remains to be established in future studies incorporating formal dysplasia grading. Notably, the unique linear arrangement of RHEBL1-positive cells in the basal layer of precancerous lesions and peritumoral epithelium suggests that RHEBL1 expression may be an early event in OSCC development. The co-localization of RHEBL1, Oct4, and Sox2 at the tumor-stroma interface in OSCC samples further supports the functional significance of this regulatory axis in cancer progression. This specific spatial distribution pattern is similar to the epithelial–mesenchymal transition zones commonly found in invasive cancers, which typically enrich cancer stem cell-like cells (Filippi et al. 2025; Hochedlinger 2006). The findings presented herein suggest that the Oct4-Sox2-RHEBL1 regulatory network may play a key role in maintaining the stem cell-like phenotype at the invasive front, thereby potentially contributing to tumor progression. Direct evidence for enhanced invasion and metastasis capability through functional assays (e.g., transwell invasion or in vivo metastasis models) remains to be established in future studies.

RHEBL1 overexpression in immortalized oral epithelial cells (*hTERT*$^{+}$*-OME*) significantly enhanced sphere formation and successfully induced tumor development in immunodeficient mice, demonstrating its potent oncogenic potential. Conversely, *RHEBL1* knockout in Cal27 cells significantly reduced sphere formation and in vivo tumorigenicity, further confirming the role of RHEBL1 in maintaining the malignant phenotype of established OSCC cells. These findings are consistent with previous reports on the role of RHEBL1 in other malignancies such as renal clear cell carcinoma and leukemia (Bailey et al. 2014; Temraz et al. 2015). However, the present study is the first to demonstrate the specific oncogenic role of RHEBL1 in OSCC and to establish its regulation by pluripotency factors Oct4 and Sox2. Notably, RHEBL1 expression levels were spontaneously upregulated in control *hTERT*$^{+}$*-OME* cells under 3D-culture conditions, suggesting that microenvironmental factors related to cell-cell interactions or altered mechanotransduction in spheroid structures may also be involved in regulating RHEBL1 expression. However, Oct4 and Sox2 protein levels were not evaluated under 3D culture conditions in the current study. Given the known ability of 3D spheroid culture to enhance stem-like characteristics, it is possible that endogenous Oct4/Sox2 levels are also upregulated in this context, contributing to RHEBL1 induction independently of exogenous overexpression. This represents an important mechanistic question for future investigation. Furthermore, this environmental shift-induced upregulation suggests that RHEBL1 may play a critical role in cellular reprogramming in response to microenvironmental cues. The 3D architecture likely creates unique cell–cell and cell–matrix interactions that activate RHEBL1 expression, potentially enhancing cellular pluripotency

and stemness properties. This phenomenon mirrors the in vivo situation at tumor invasion fronts, where cells experience significant changes in their physical and biochemical environment. The ability of RHEBL1 to respond to these environmental transitions may represent a key mechanism through which cancer cells adapt to new microenvironments and acquire the plasticity needed for invasion and metastasis. This aligns with emerging evidence emphasizing the importance of microenvironmental factors in regulating cancer stem cell properties (Cai et al. 2016; Nishi et al. 2014). It should be noted that the current study did not assess immune infiltration or immune-related markers in OSCC tissues or animal models, which represents an important limitation. Future studies should investigate the relationship between the Oct4-Sox2-RHEBL1 axis and the tumor immune microenvironment, as this interaction may further illuminate the role of this regulatory axis in immune evasion and tumor progression.

Oct4 and Sox2 cooperatively activated *RHEBL1* transcription by directly binding to two conserved motifs within its promoter region. This synergistic action is consistent with the established model of Oct4-Sox2 complex formation, in which these factors interact to regulate pluripotency gene expression in embryonic stem cells (Bonneau and Parmar 2012; Moyo et al. 2017). ChIP-PCR confirmed the direct binding of Oct4 and Sox2 to the *RHEBL1* promoter in OSCC cell lines, providing strong evidence for the role of this regulatory mechanism in oral carcinogenesis. This finding significantly expands our understanding of how pluripotency factors promote tumor development by activating specific oncogenic signaling pathways.

The identification of the Oct4-Sox2-RHEBL1 regulatory axis in OSCC has important implications for both prognostic assessment and therapeutic intervention. The specific expression patterns of these factors in precancerous lesions and at the invasive front of OSCC suggest that they may serve as biomarkers for early detection and risk stratification. Future studies should assess whether RHEBL1 expression, either alone or in combination with Oct4 and Sox2, can predict the risk of malignant transformation in potentially malignant oral disorders. From a therapeutic perspective, targeting the Oct4-Sox2-RHEBL1 pathway represents a promising strategy for OSCC treatment. We also acknowledge that the current study did not systematically correlate RHEBL1, Oct4, or Sox2 expression levels with detailed clinical parameters such as tumor stage, lymph node involvement, or patient survival outcomes, partly due to limited clinical annotation in the commercial tissue microarray used. Future prospective studies with well-annotated clinical cohorts are needed to establish the prognostic value of the Oct4-Sox2-RHEBL1 axis in OSCC.

From a mechanistic perspective, RHEBL1 may also interact with inflammatory pathways critical to cancer development. The NF-κB signaling pathway plays a key role in OSCC pathogenesis (Moyo et al. 2017; Du et al. 2023), and RHEBL1 has been reported to activate NF-κB transcriptional activity (Yuan et al. 2005). The spontaneous upregulation of RHEBL1 observed in 3D culture conditions is consistent with our previous observation of p65 nuclear translocation in hTERT+-OME cells under 3D conditions (Qiao et al. 2012), suggesting a potential connection between RHEBL1 and NF-κB activation in the tumor microenvironment context. However, the precise mechanistic relationship between RHEBL1 and NF-κB in OSCC requires direct experimental validation in future studies.

Although this study demonstrated the functional significance of RHEBL1 in OSCC development, the exact molecular mechanisms by which RHEBL1 exerts its oncogenic effects remain to be more comprehensively elucidated. Future research should focus on investigating specific downstream pathways activated by RHEBL1 in OSCC cells, with particular attention to key regulatory axes such as mTOR signaling, c-Myc activation, and NF-κB transcriptional activity, with the aim of developing precision therapeutic strategies targeting this pathway.A key limitation of the current study is the absence of rescue experiments in which RHEBL1 is re-expressed in Oct4/Sox2-knockdown cells to confirm that RHEBL1 mediates the observed tumorigenic and stemness phenotypes downstream of Oct4/Sox2. Such experiments are critical to formally establish the epistatic relationship within this regulatory axis and represent a priority for future investigation.

Conclusions

This investigation established a crucial regulatory relationship between Oct4, Sox2, and RHEBL1 in OSCC development. Through comprehensive bioinformatic analysis and clinical sample validation, significant correlation patterns were found between these factors in both OSCC and precancerous lesions. Genetic modification of *RHEBL1* revealed its direct influence on cellular proliferation in both normal oral epithelial and OSCC cells. The mechanistic studies uncovered that Oct4 and Sox2 function as synergistic transcriptional regulators of *RHEBL1*, thereby controlling oral squamous cell proliferation. These findings advance our understanding of OSCC pathogenesis and identify the Oct4-Sox2-RHEBL1 axis as a potential therapeutic target for OSCC treatment.

Glossary

OSCC (Oral squamous cell carcinoma)	A malignant tumor originating from the epithelium of the oral mucosa
RHEBL1 (Ras homolog enriched in brain like 1)	Also known as RHEB2, member of the Ras superfamily, plays a key role in cell proliferation and tumor development
Oct4 (Octamer-binding transcription factor 4)	Also known as POU5F1, a POU family transcription factor crucial in embryonic development and stem cell maintenance
Sox2 (Sex determining region Y-box 2)	B1 subgroup member of the Sox family, essential for embryonic development and stem cell properties
hTERT (Human telomerase reverse transcriptase)	Maintains telomere length, conferring immortalization characteristics to cells
NOM (Non-neoplastic histologically normal oral mucosa)	Normal oral mucosa tissue without neoplastic changes
OLP (Oral lichen planus)	A potentially malignant disorder of the oral cavity
OLK (Oral leukoplakia)	A potentially malignant white patch or plaque on the oral mucosa
OME (Oral mucosal epithelial cell line)	Cell line derived from oral mucosal epithelium
mTOR (Mammalian target of rapamycin)	Key signaling pathway that regulates cell growth, proliferation, and survival
NF-κB (Mammalian target of rapamycin)	Mammalian target of rapamycin Transcription factor that regulates inflammatory responses and immune function
IRF3 (Interferon regulatory factor 3)	Involved in innate immune responses
POU (Pit-Oct-Unc)	A class of DNA-binding domains present in various transcription factors
HMG (High mobility group)	A class of proteins that bind to DNA
FGF4 (Fibroblast growth factor 4)	Signaling molecule involved in embryonic development
RAX (Retina and anterior neural fold homeobox)	Transcription factor involved in eye development
NOD-SCID (Non-obese diabetic-severe combined immunodeficiency)	Immunodeficient mouse model used for xenograft studies
CRISPR-Cas9 (Clustered regularly interspaced short palindromic repeats-CRISPR-associated protein 9)	Gene editing technology that allows precise modification of DNA sequences
RT-qPCR (Reverse transcription quantitative polymerase chain reaction)	Technique used to detect and quantify specific RNA expression
ChIP-PCR (Chromatin immunoprecipitation-polymerase chain reaction)	Technique used to detect protein-DNA interactions
DMEM/F12 (Dulbecco's modified Eagle medium/nutrient mixture F-12)	Cell culture medium used for growing various cell types
FPKM (Fragments per kilobase of transcript per million mapped reads)	Method for normalizing RNA-seq data
RPKM (Reads per kilobase of transcript per million mapped reads)	Method for normalizing RNA-seq data
RIPA buffer (Radioimmunoprecipitation Assay buffer)	Used for protein extraction from cells and tissues
bFGF (Basic fibroblast growth factor)	Cytokine that promotes cell proliferation
EGF (Epidermal growth factor)	Cytokine that promotes cell proliferation
B27 (B27 supplement)	Maintains neuronal and stem cell growth in serum-free media
GAPDH (Glyceraldehyde 3-phosphate dehydrogenase)	Commonly used as an internal reference gene
NCBI (National Center for Biotechnology Information)	Provides access to biomedical and genomic information
UCSC (University of California Santa Cruz)	Provides genome browser and bioinformatics tools
JASPAR (JASPAR database)	Database of transcription factor binding sites
IKK (IκB kinase)	Key enzyme in the NF-κB signaling pathway

IκB (Inhibitor of κB)	Protein that regulates NF-κB activity
TBK1 (TANK-binding kinase 1)	Protein kinase involved in innate immune responses
c-Myc (Cellular myelocytomatosis)	Proto-oncogene transcription factor

Supplementary Information The online version contains supplementary material available at https://doi.org/10.1007/s10142-026-01942-9.

Acknowledgements Most of the research was carried out in the High Incidence Disease Prevention and Treatment Pharmacology Key Laboratory, Guilin Medical University, Guilin, China. We would like to thank the staff of Laboratory (Kefeng Zhang) for their kind and professional help.

Author contributions Conceptualization: F.Q., B.Q., Q.J.Methodology: F.Q., Q.J.Investigation: F.Q., Y.C., P.L., X.S., Y.L.Formal Analysis: F.Q.Data Curation: Y.C., P.L., X.S., Y.L.Resources: Z.C., A.L.Writing – Original Draft: Y.C.Writing – Review & Editing: Z.C., A.L., B.Q., Q.J.Supervision: B.Q., Q.J.Project Administration: B.Q., Q.J.Visualization: F.Q.,Y.C, Y.L, Z.C.Funding Acquisition: F.Q., Q.J.

Funding This research was supported by the Affiliated Stomatology Hospital of Guilin Medical University (2022kqrc-01) and the Education Department of Guangxi Zhuang Autonomous Region (2024KY0499). The funding agency had no role in the study design; in the collection, analysis, and interpretation of the data; in the writing of the report; and in the decision to submit the article for publication.

Data availability The datasets used and analyzed in the current study are available from the corresponding author on reasonable request.

Declarations

Ethics approval This study was approved by the Ethics Committee of Guilin Medical University (No: GLMC20240305) and conducted in accordance with the Declaration of Helsinki. Experimental animals were purchased from Beijing Weitong Lihua Experimental Animal Technology Co., Ltd., with the license number SCXK (Jing) 2016-0006. All breeding and experimental procedures strictly followed the guidelines set by the Zhengzhou University Experimental Animal Ethics Committee.

Consent to participate All patients provided written informed consent for the collection and storage of their tissues for research purposes.

Competing interests The authors declare no competing interests.

References

Al H (2023) Immunotherapy, chemotherapy, or both: options for first-line therapy for patients with recurrent or metastatic head and neck squamous cell carcinoma. J Clin Oncol 41:736–741. https://doi.org/10.1200/jco.22.01408

Alevizopoulos K, Vlach J, Hennecke S, Amati B (1997) Cyclin E and c-Myc promote cell proliferation in the presence of p16INK4a and of hypophosphorylated retinoblastoma family proteins. EMBO J 16:5322–5333. https://doi.org/10.1093/emboj/16.17.5322

Aspuria P, Tamanoi F (2004) The Rheb family of GTP-binding proteins. Cell Signal 16:1105–1112. https://doi.org/10.1016/j.cellsig.2004.03.019

Bailey S, Zhou B, Damrauer J, Krishnan B, Wilson H, Smith A et al (2014) mTOR inhibition induces compensatory, therapeutically targetable MEK activation in renal cell carcinoma. PLoS One 9:e104413. https://doi.org/10.1371/journal.pone.0104413

Bonneau A, Parmar N (2012) Effects of RhebL1 silencing on the mTOR pathway. Mol Biol Rep 39:2129–2137. https://doi.org/10.1007/s11033-011-0960-6

Cai J, He B, Li X, Sun M, Lam A, Qiao B et al (2016) Regulation of tumorigenesis in oral epithelial cells by defined reprogramming factors Oct4 and Sox2. Oncol Rep 36:651–658. https://doi.org/10.3892/or.2016.4851

Chen K, Hsieh M, Lin YY, Chen M, Lien M, Yang S et al (2022) Visfatin polymorphisms, lifestyle risk factors and risk of oral squamous cell carcinoma in a cohort of Taiwanese males. Int J Med Sci 19:762–768. https://doi.org/10.7150/ijms.69868

Du Y, Yang Y, Zhang W, Yang C, Xu P (2023) Human β-defensin-3 and nuclear factor-kappa B p65 synergistically promote the cell proliferation and invasion of oral squamous cell carcinoma. Transl Oncol 27:101582. https://doi.org/10.1016/j.tranon.2022.101582

Filippi A, Deculescu-Ioniță T, Hudiță A, Baldasici O, Gălățeanu B, Mocanu M (2025) Molecular mechanisms of dietary compounds in cancer stem cells from solid tumors: insights into colorectal, breast, and prostate cancer. Int J Mol Sci. https://doi.org/10.3390/ijms26020631

Gao Y, Tan D, Girbig M, Hu H, Zhou X, Xie Q et al (2024) The emergence of Sox and POU transcription factors predates the origins of animal stem cells. Nature Communications 15:9868. https://doi.org/10.1038/s41467-024-54152-x

Gilligan G, Panico R, Lazos J, Morelatto R, Belardinelli P, Criscuolo M et al (2024) Oral squamous cell carcinomas and oral potentially malignant disorders: a Latin American study. Oral Dis 30:2965–2984. https://doi.org/10.1111/odi.14778

Grimm D, Bauer J, Wise P, Krüger M, Simonsen U, Wehland M et al (2020) The role of SOX family members in solid tumours and metastasis. Semin Cancer Biol 67:122–153. https://doi.org/10.1016/j.semcancer.2019.03.004

Hochedlinger K, Jaenisch R (2006) Nuclear reprogramming and pluripotency. Nature 441:1061–1067. https://doi.org/10.1038/nature04955

Liu W, Shen X, Shen Z (2025) A scientometric study on research trends and characteristics of oral leukoplakia and oral lichen planus. Journal of Dental Sciences 20:672–677. https://doi.org/10.1016/j.jds.2024.08.025

Moyo T, Wilson C, Moore D, Eischen C (2017) Myc enhances B-cell receptor signaling in precancerous B cells and confers resistance to Btk inhibition. Oncogene 36:4653–4661. https://doi.org/10.1038/onc.2017.95

Nishi M, Sakai Y, Akutsu H, Nagashima Y, Quinn G, Masui S et al (2014) Induction of cells with cancer stem cell properties from nontumorigenic human mammary epithelial cells by defined reprogramming factors. Oncogene 33:643–652. https://doi.org/10.1038/onc.2012.614

Qiao B, He B, Cai J, Yang W (2014) The expression profile of Oct4 and Sox2 in the carcinogenesis of oral mucosa. Int J Clin Exp Pathol 7:28–37

Qiao B, Gopalan V, Chen Z, Smith R, Tao Q, Lam A (2012) Epithelial-mesenchymal transition and mesenchymal-epithelial transition are essential for the acquisition of stem cell properties in hTERT-immortalised oral epithelial cells. Biol Cell 104:476–489. https://doi.org/10.1111/boc.201100077

Sato T, Mukai S, Ikeda H, Mishiro-Sato E, Akao K, Kobayashi T et al (2021) Silencing of SmgGDS, a novel mTORC1 inducer that binds to RHEBs, inhibits malignant mesothelioma cell proliferation. Mol Cancer Res 19:921–931. https://doi.org/10.1158/1541-7786.Mcr-20-0637

Temraz S, Mukherji D, Shamseddine A (2015) Dual inhibition of MEK and PI3K pathway in KRAS and BRAF mutated colorectal cancers. Int J Mol Sci 16:22976–22988. https://doi.org/10.3390/ijms160922976

Tian Y, Shen L, Li F, Yang J, Wan X, Ouyang M (2020) Silencing of RHEB inhibits cell proliferation and promotes apoptosis in colorectal cancer cells via inhibition of the mTOR signaling pathway. J Cell Physiol 235:442–453. https://doi.org/10.1002/jcp.28984

Tsai S, Clavel C, Kim S, Ang Y, Grisanti L, Lee D et al (2010) Oct4 and klf4 reprogram dermal papilla cells into induced pluripotent stem cells. Stem Cells 28:221–228. https://doi.org/10.1002/stem.281

Wang W, Chien Y, Wong Y, Lin Y, Lin J (2012) Effects of KRAS mutation and polymorphism on the risk and prognosis of oral squamous cell carcinoma. Head Neck 34:663–666. https://doi.org/10.1002/hed.21792

WHO (2017) Classification of Head and Neck Tumours (ed) PJ E-NACJGJTTS

Xiao B, Zuo D, Hirukawa A, Cardiff RD, Lamb R, Sonenberg N et al (2020) Rheb1-independent activation of mTORC1 in mammary tumors occurs through activating mutations in mTOR. Cell Rep 31:107571. https://doi.org/10.1016/j.celrep.2020.107571

Yang Z, Cui Y, Ni W, Kim S, Xuan Y (2017) Gli1, a potential regulator of esophageal cancer stem cell, is identified as an independent adverse prognostic factor in esophageal squamous cell carcinoma. J Cancer Res Clin Oncol 143:243–254. https://doi.org/10.1007/s00432-016-2273-6

Yu J, Moon E, Kim J, Koo J (2023) Identification of small GTPases that phosphorylate IRF3 through TBK1 activation using an active mutant library screen. Biomol Ther 31:48–58. https://doi.org/10.4062/biomolther.2022.119

Yuan J, Shan Y, Chen X, Tang W, Luo K, Ni J et al (2005) Identification and characterization of RHEBL1, a novel member of Ras family, which activates transcriptional activities of NF-kappa B. Mol Biol Rep 32:205–214. https://doi.org/10.1007/s11033-005-0984-x

Zanoni D, Montero P, Migliacci J, Shah J, Wong R, Ganly I et al (2019) Survival outcomes after treatment of cancer of the oral cavity (1985–2015). Oral Oncol 90:115–121. https://doi.org/10.1016/j.oraloncology.2019.02.001